Effect of Temperature on Electrochemical Behavior of Cobalt Diselenide Ternary Composite-based Supercapacitor

Shweta Tanwar[1], Nirbhay Singh[2], Anurag Gaur[1*], A.L Sharma[3*]

[1]*Department of Physics, Netaji Subhas University of Technology, Delhi-110078, India*

[2]*Department of Applied Physics, Amity School of Engineering and Technology, Amity University Gwalior Madhya Pradesh-474005, India*

[3]*Department of Physics, Central University of Punjab, Bathinda, Punjab-151401, India*

Volume 1, Issue 6, December 2024
Received:27 September, 2024; Accepted: 29 November, 2024
DOI: https://doi.org/10.63015/10s-2444.1.6

**Corresponding Author Email: anurag.gaur@nsut.ac.in; alsharma@cup.edu.in*

Abstract: The electrochemical behavior of a cobalt diselenide ($CoSe_2$)-based ternary composite for hybrid supercapacitor applications across varying temperatures has been studied. To get advanced electrochemical results composite was synthesized by incorporating activated carbon and cellulose fibers with $CoSe_2$ (the optimization of the ternary composite is depicted in our other research paper). A series of electrochemical analyses was directed at different temperatures to assess the temperature-dependent behavior of the supercapacitor. The results demonstrate that the ternary composite exhibits enhanced electrochemical properties, with a high specific capacitance at 40˚C temperatures due to improved ion mobility and charge transfer kinetics. At 40°C, the composite-based cell revealed a specific capacitance of 248 F g^{-1}, which further decreased at higher temperatures, showcasing a negative correlation between temperature and electrochemical performance. The energy and power densities obtained for the same are 22 Wh kg^{-1} and 411 W kg^{-1}. The findings suggest that such hybrid supercapacitors could play a dynamic part in energy storage technologies.

1. Introduction: The society is currently grappling with energy storage [1]. This situation is driven by several factors, including the limitations of renewable energy resources and the increasing energy demand due to population growth, among others. Conventional, energy sources (non-renewable) including fossil fuels are reducing speedily, prompting the scientific community to explore renewable energy as a sustainable alternative [2]. While renewable energy offers numerous advantages, it is not consistently reliable. However, this reliability can be improved through the development of energy storage devices. These devices help store energy generated from renewable sources, ensuring a steady supply during peak demand. Among the most common energy storage solutions are secondary batteries and supercapacitors [3]. Supercapacitors (SC), in particular, have gained popularity due to their benefits, including high reliability, cost-effectiveness, fast charge/discharge rates, excellent steadiness, high power density, and safety in use. Conventional supercapacitors are made of three main parts: a separator, electrolyte, and electrode [4]. Despite their advantages, supercapacitors face the disadvantage of low energy density of low value, which needs to be addressed in the future [5]. For

supercapacitors, the energy density is determined by its potential window and capacitance, as calculated using the formula $E=0.5CV^2$ (Wh kg^{-1}) [6]. Both the potential window and capacitance hinge on the intrinsic assets of the electrode and electrolyte. Aqueous supercapacitors, based on their working machinery, are characterized as electric double-layer capacitors (EDLCs) and pseudocapacitors [7]. Hybrid SC, a third type, syndicates the profits of both EDLCs and pseudocapacitors while addressing issues such as low capacitance and energy density, and poor stability [8]. One way to improve the potential window is by designing electrode materials that can store charges through redox reactions. Electrode materials with unique morphologies, large surface areas, and favourable microstructures can significantly enhance a supercapacitor's capacitance [9].

Transition metal diselenides (MSe_2), where "M" can represent various transition metals have emerged as promising electrode materials for supercapacitors. Their popularity stems from characteristics like high area (surface), wide range oxidation states, low electronegativity, exceptional morphologies, and multifunctional electrical structures [10]. Commonly used MSe_2 compounds in supercapacitors include $CoSe_2$. For instance, Chen et al. synthesized a $CoSe_2$ electrode via a thermal method, achieving 554 F g^{-1} and a density (energy) of approximately 20 Wh kg^{-1} with a 1.7 V potential window [11]. However, pure $CoSe_2$ materials suffer from drawbacks such as low electronic conductivity, and limited capacitance. To overcome these limitations, researchers develop composite carbon-based materials. These carbon materials offer high surface area, admirable electronic conductivity, and boosted stability [12]. Notable studies in this area include Yu et al., who prepared a $CoSe_2$@carbon composite using a hydrothermal method, delivering 332 mF cm^{-2} capacitance and 95% cyclic stability [13]. Despite these improvements, binary $CoSe_2$-carbon binary composites often experience agglomeration, complicating the electrolyte ion transport and insertion/extraction processes. To address this issue, the introduction of dispersants is needed to reduce aggregation, enhance electrolyte wettability, and shorten the dispersion path for ions of the electrolyte.

In this study, we assume that incorporating cellulose into cobalt diselenide composites can effectively reduce agglomeration, facilitate electron mobility by providing easy diffusion pathways, and improve electrochemical performance, particularly energy density and stability. Cellulose, being abundant, biocompatible, biodegradable, and mechanically stable, offers an improved surface area and abundant active locations, assembly it a perfect candidate for this role. To prevent clustering in $CoSe_2$-carbon nanocomposites we have utilized cellulose in this work. This paper presents the preparation of cellulose-incorporated ternary composites based on cobalt diselenides, using a room-temperature physical mixing approach (optimization of the ternary composite is depicted in our previous reports [1]). The objective of this study is to study the temperature effect on the electrochemical behavior of the designed supercapacitor based on a ternary composite of cobalt diselenide. Thus, the electrochemical behavior of the symmetric cell designed has been studied for various temperature ranges from 40 to 120˚C.

2. Experimental Segment

2.1. Materials

The chemicals utilized for this study were procured from Sigma Aldrich as ACS-grade reagents and were used directly for synthesis without further purification. The materials include hydrazine hydrate ($N_2H_4 \cdot H_2O$), potassium hydroxide (KOH) pellets, Activated carbon (AC), selenium (Se) powder, polyvinylidene fluoride (PVDF), N-methyl-2-pyrrolidone (NMP), carbon black, and cobalt

nitrate hexahydrate (Co $(NO_3)_2 \cdot 6H_2O$). Cellulose fiber (Sigma Aldrich, product number C6288) was used with a density of 0.600 g/cm³. The moisture content of the cellulose fiber was at least 10%. Double-distilled water (DDW) was used throughout the sample preparation process.

2.2 Synthesis of Cobalt diselenide ternary composite

The binary composites of $CoSe_2$, along with activated carbon (AC), were produced employing the hydrothermal technique as described in this report [14]. The ternary composites were prepared by physically blending the above-prepared binary composites with cellulose. Cellulose (weight percentage 5%), was incorporated into the binary composite matrix, and the blend was moved continuously for 6 hours. The resultant sample was dried in a controlled oven at 70°C for 12 hrs. The final samples were designated as CAC-40 for further analysis. The flowchart for the ternary composite preparation process is shown in **Fig. 1**. The reaction kinetics for the formation of the binary composites were detailed in one of our previous research articles [14]. The activated carbon coating on the pure $CoSe_2$ was designed to enhance stability and increase the area of the surface for pure $CoSe_2$.

2.3 Characterization tools used

X-ray diffraction (XRD) data was extracted by a PANalytical Empyrean diffractometer. The XRD curves were recorded over a 2θ range of 10 to 70 degrees. Fourier transform infrared (FTIR) spectra were attained by NEXUS-870 spectrometer, over 600-4000 cm^{-1}. The morphology was observed using a Merlin Compact system. The surface area cum pore size distribution was done by using the nitrogen adsorption-desorption technique with a BELSORP-maxII instrument (MicrotracBEL Corporation). The thermal steadiness of the manufactured sample was measured using thermogravimetric analysis (TGA) on a SHIMADZU DTG-60H instrument. The analysis was conducted under dynamic temperature ranging from 30°C to 550°C, in a nitrogen (N_2) atmosphere at 10°C/min (constant heating rate). Differential scanning calorimetry (DSC) was executed using a DSC-Sirius 3500 instrument from 30°C to 500°C, under a N_2 atmosphere at 10°C/min (sustained heating rate).

2.4 Electrochemical investigation

The electrodes of the organized composite material were fabricated by spread over a slurry paste onto a nickel (Ni) foam current collector, then dried at 60°C in an oven for several hours. The slurry was prepared by homogeneously mixing in a ratio of 80: 10: 10 (active material, PVDF binder, and carbon black (CB) in a solvent NMP. The mass of the active material was 3 mg coated on Ni foam (diameter of 1 cm). A symmetric cell was assembled to evaluate the electrochemical properties of the sample (prepared) in a two-electrode (2-E) system. The symmetric cell was created by placing a filter paper soaked in a few drops of 6 M KOH electrolyte between two identical electrodes. The assembled cell

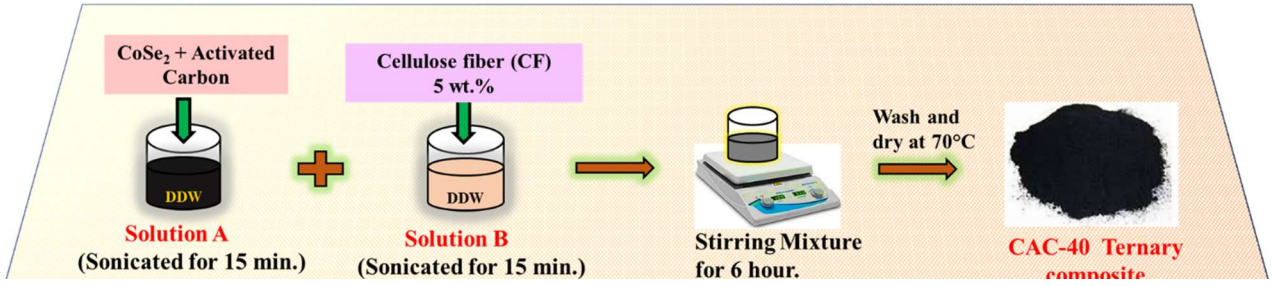

Figure 1. Schematic depiction of preparation of $CoSe_2$-based ternary composite.

can be represented symbolically as Electrode//Electrolyte//Electrode. The cell was further used for electrochemical testing.

The electrochemical analysis, like cyclic voltammetry (CV), galvanostatic charge-discharge (GCD), cum electrochemical impedance spectroscopy (EIS), was run on the symmetric cell via a 2-E (electrode) configuration. A CHI760E instrument was employed for these measurements. Whatman filter paper, with KOH (6M), was used as the separator. The use of a highly concentrated electrolyte was chosen due to the small size of OH^- ions, which results in high mobility and conductivity, thereby enhancing the electrochemical properties. CV and GCD readings were recorded over a potential range of -0.8 V to 0.8 V at varying scan rates and current densities. EIS data were taken across a frequency range of 1 Hz to 0.1 MHz, using a constant voltage of 5 mV. The following formulae were employed for calculating energy density, specific capacitance, and power density given below [15]:

Specific Capacitance

Using CV, $C_{S-CV} = \frac{\int iVdV}{m*v*\Delta V}$ (F g^{-1}) (1)

GCD, $C_s = \frac{2*i*\int V\,dt}{m(\Delta V)^2}$ (F g^{-1}) (2)

Energy density

From GCD, $E = \frac{C*V^2}{7.2}$ (Wh kg^{-1}) (3)

and Power density

$P = \frac{E*3600}{t_d}$ (W kg^{-1}) (4)

Here *m, v, V,* t_d*, and I,* are related to mass, scan rate, potential window, time of discharging, and current independently.

3. Results and discussion

3.1 Structural, Chemical, and Surface Analysis

The successful synthesis of the organized material was achieved through X-ray diffraction. **Fig. 2a** illustrates the XRD plot for pure AC, cobalt diselenide, cellulose, and the ternary composite (CAC-40). Cellulose fiber was merged into the binary composite which contains $CoSe_2$ and activated carbon (1:1). Additionally, 5% by weight of cellulose fiber was added to the binary composite of $CoSe_2$ and activated carbon. Two broad peaks at 25° and 43° correspond to crystalline planes of the activated carbon used. The $(1\bar{1}0)$, (110), (200), and (004) planes connected to cellulose fiber show peaks at 15.1°, 16.2°, 22.7°, and 34.3°. In the XRD pattern for pure $CoSe_2$, peaks observed agree with the planes, matching the JCPDS card No. 053-0449. These peaks indicate the formation of the orthorhombic phase associated with $CoSe_2$, with lattice parameters 3.628 Å, 4.85 Å, and 5.827 Å [16]. The XRD pattern for sample CAC-40 authorizes the creation of the required composite.

The chemical atmosphere and validation of bonds cum groups in the synthesized ternary composite were investigated using the FTIR tool. **Fig. 2b** presents the FTIR bands for carbon, cellulose, cobalt diselenide, and prepared composite for 600 to 4000 cm^{-1} wavenumber. The bands for ranges like 690-720 cm^{-1} and 800–850 cm^{-1} are accredited to O-Co-O vibrations cum Co-Se bonding [17]. Bands corresponding to C-O and C=O groups appeared at 1130 cum 1581 cm^{-1}. Peaks at 1050 cm^{-1} and 1648 cm^{-1} relating to C-O-C and -COO- stretching are for cellulose, while the -COO- band indicates the cellulose's electronegativity and dispersibility in water [18]. Peaks around 1539 cm^{-1}, cobalt (Co) complex. Bands around 2900 cm^{-1} correspond to C-H functional groups in samples [19]. Broad peaks about 3000–3320 cm^{-1} and 3350–3500 cm^{-1} regions are credited to OH groups in the samples [1].

The surface area along with pore size for the composite samples was examined using isotherms methods (nitrogen adsorption-desorption). **Fig. 2c** illustrates the BET plot for

the prepared samples. The isotherm for the CAC-40 sample resembles a type-IV curve, indicating a mesoporous structure in the ternary composite. The pore size for this CAC-40 ranges from 0 to 160 nm. The N_2 adsorption/desorption scheme, along with the inset showing the pore size distribution arc for the CAC-40 sample, is presented in **Fig. 2c**. The area at the surface of CAC-40 was estimated to be 460 m^2 g^{-1}, with a pore diameter of around 4.1 nm. The BET results suggest that the CAC-40 ternary composite has a larger surface area, which could enhance the storage of the charges at both the outer and internal active sites. As a result, the CAC-40 sample is expected to demonstrate excellent electrochemical performance.

3.2 Temperature related studies

The stability with temperature variation of the CAC sample was verified through the Thermo-gravimetric analysis (TGA) tool. Initially, a weight reduction of approximately 2.6 % below 200 °C indicates the evaporation of moisture from the exterior area of the sample elements. Subsequently, a weight reduction of about 34.6 % is detected over the temperature range of 200 to 570 °C, reflecting the devolatilization of the material. As the TGA readings were conducted under an inert nitrogen atmosphere, the likelihood of oxidation or combustion of the constituents (such as cobalt, selenium, and carbon) in the sample is minimal. Consequently, we spot a

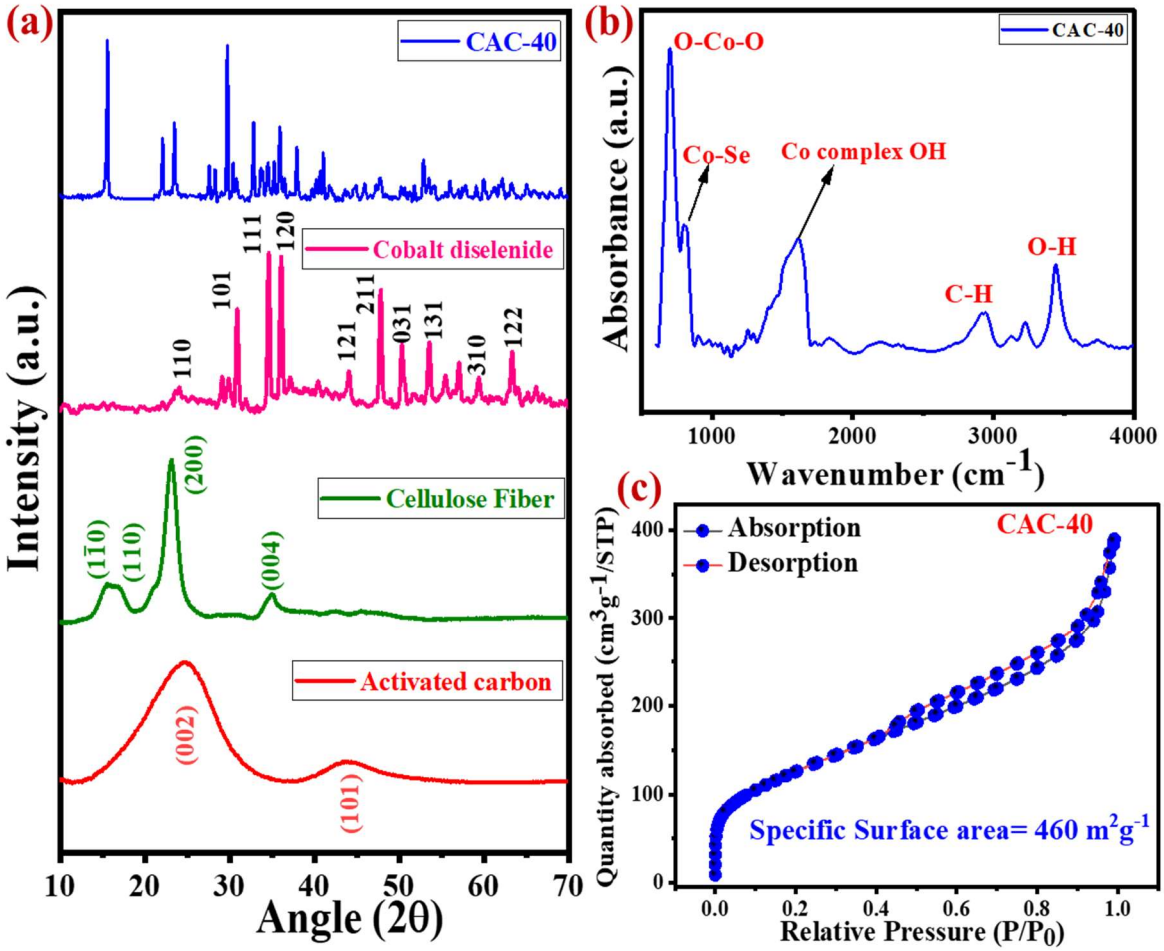

Figure 2. (a) X-ray diffraction, (b) FTIR plot, and (c) nitrogen adsorption-desorption isotherms for CAC-40 sample.

nonstop decay in the TGA curve through the complete temperature region.

DSC was employed to authorize the upsurge of conductivity (electrical) which is due to a growth of ions (free) and a reduction of crystallinity. **Fig.3b** shows the DSC results for the CAC-40 sample. The endothermic peak observed over the 0-300˚ C temperature range is accredited to the melting point of different components (selenium, carbon which is activated, and cellulose fiber) of the prepared composite. The exothermic peaks from 300-500˚ C temperature represent crystallization and the reaction of different components to formulate the ternary composite.

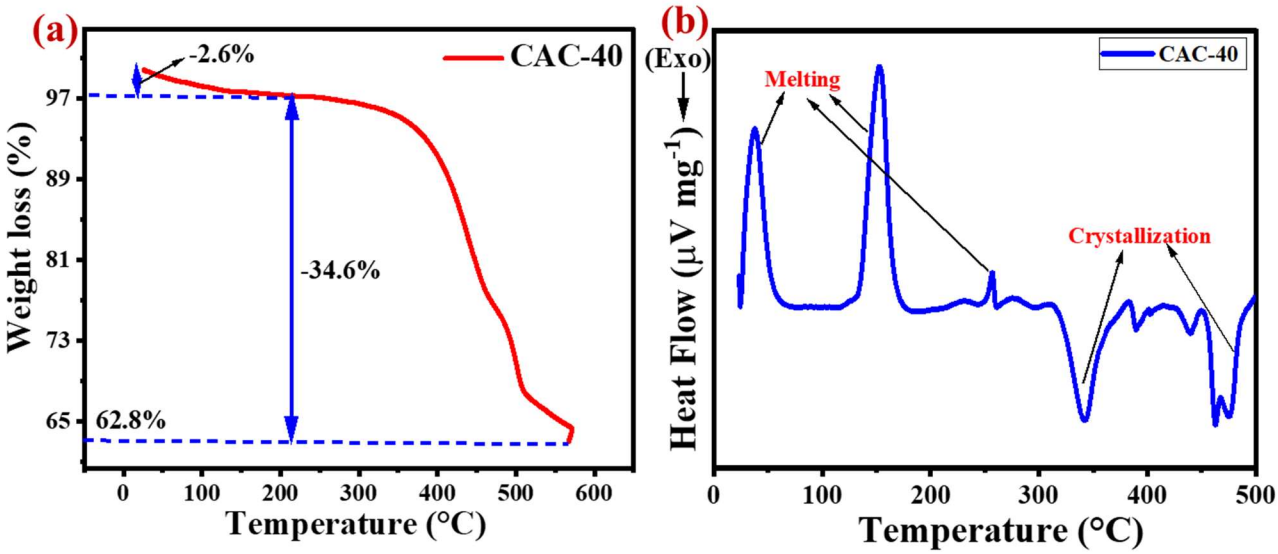

Figure 3. (a) TGA, and (b) DSC for CAC-40 sample.

3.3 Morphology study via field emission scanning electron microscopy-FESEM

To explore the morphology of the ternary composite (CAC-40), we conducted an investigation using FESEM.

Fig.4 presents the FESEM pictures for the CAC-40 sample. The images reveal intact $CoSe_2$ particles enveloped by spherical activated carbon, with cellulose fibers visible throughout the structure. Additionally, the flakes of $CoSe_2$ are uniformly distributed and attached to the activated carbon. Our previous report outlined the rationale for coating $CoSe_2$ particles with activated carbon. The addition of cellulose fibers to the $CoSe_2$ and carbon composite was aimed at preventing the aggregation of $CoSe_2$ particles, creating a biodegradable and less contaminated material, and ensuring mechanical stability. This design optimizes the architecture of the composite to achieve a high area at the surface and a clear circulation path for ions associated with electrolytes, facilitating efficient charge storage.

3.4 Electrochemical investigation of the prepared cell for different temperature

The electrochemical properties of a composite made of $CoSe_2$ with cellulose were examined using a 2-E configuration at 1.6 V (potential window) in a potassium hydroxide electrolyte of six molarity. The performance of the composite was evaluated through, GCD, EIS, and CV.

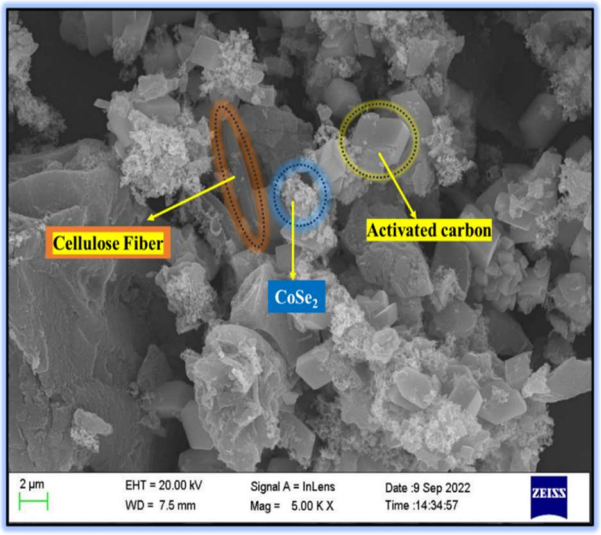

Figure 4. FESEM image for CAC-40 at 2 micrometers.

Fig. 5a presents the CV arcs of the ternary composite at dissimilar temperatures while measuring electrochemical measurements, ranging from 40°C to 120°C, with a 100-mV s^{-1} scan rate. The CAC-40 material exhibited the largest CV curve area, indicating superior performance compared to other temperature-based samples. **Fig. 5b** shows the specific capacitance (Cs), estimated using equation 1, for all cells at various temperatures at a common scan rate. **Fig.5c** illustrates the CV curve for CAC-40 at different scan rates, revealing a distorted rectangular profile. This shape suggests that charge storage occurs

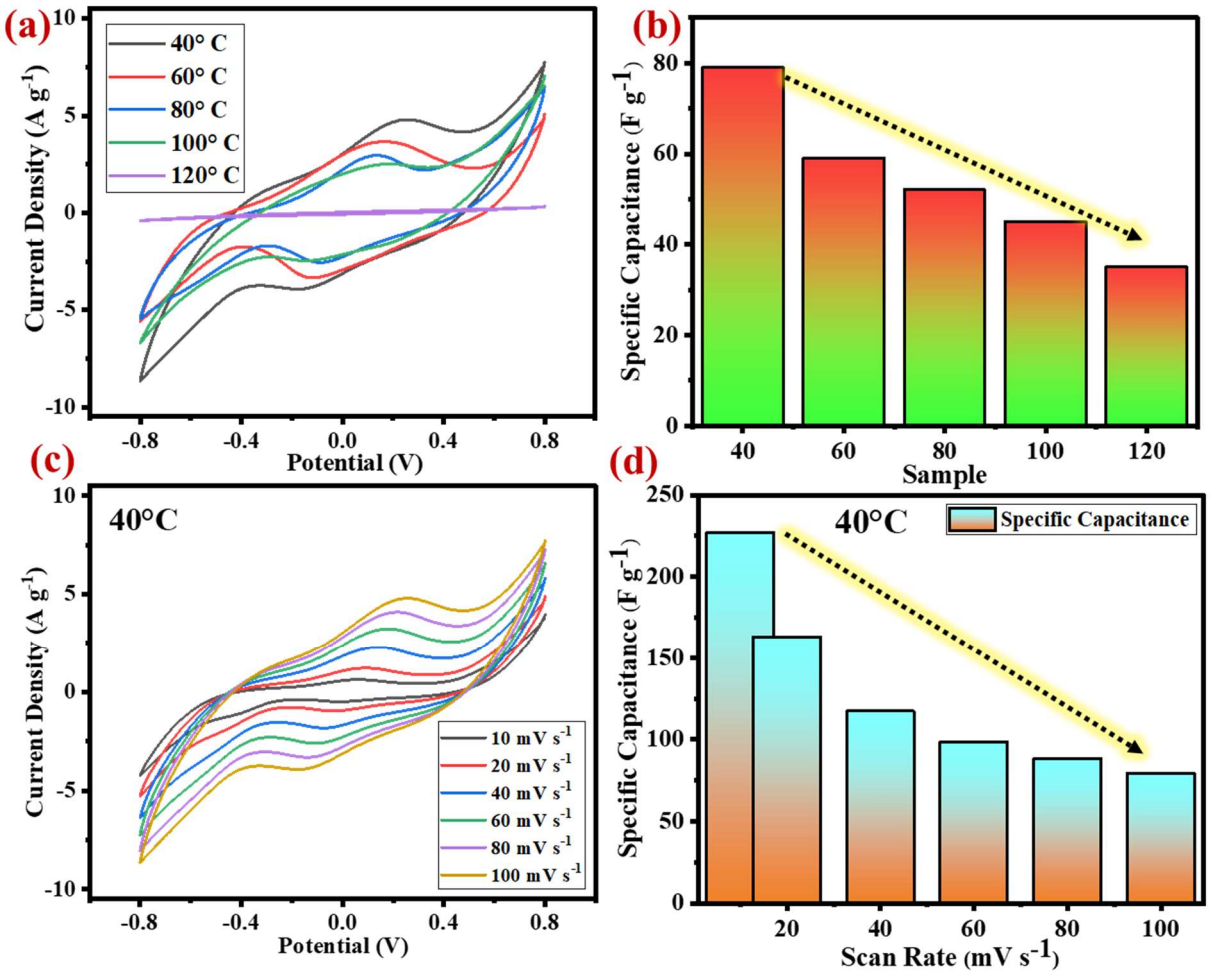

Figure 5. (a) CV plot for temperature range 40-120°C, (b) specific capacitance at 100 mV s^{-1} for the sample at changed temperature ranges, (c) CV graph for CAC-40 at unlike scan rates, and (d) variation of capacitance with scan rate for CAC-40 sample.

through two processes: (1) the adsorption of electrolytic ions at the boundary of two components, creating an EDL at the boundary, and (2) a reversible faradaic process, involving the passage of electrolytic ions inner surface of the electrode material. **Fig. 5d** displays the specific capacitance (Cs) against the scan rate (10 to 100 mV s^{-1}). The Cs value declines with increasing scan rate, likely due to reduced ion accumulation on the electrode surface at higher scan rates.

Fig. 6a presents the GCD arcs for ternary composite samples synthesized at dissimilar temperatures, at 2 A g^{-1}. The GCD curve outline deviates from the typical convention shape for all samples at different temperatures, which is attributed to the contribution of mutually formed electrostatic layer and oxidation-reduction reactions, allowing for enhanced charge storage. **Fig. 6b** shows the GCD profiles for CAC-40 at varying current densities.

The specific capacitance (C_s), calculated with equation 2 at unlike current densities (ranging from 1 to 5 A g^{-1}), is depicted in **Fig. 6c**. The drift in C_s values obtained from GCD measurements aligns with the results of CV analysis across all samples. Electrochemical parameters for all samples at varied temperatures, calculated using equations 1 to 4, are summarized in **Table 1**. A Ragone plot proving the connection between power and energy density for CAC-40 is shown in **Fig. 6d.** The CAC-5 samples demonstrated the highest performance, delivering approximately 22 Wh kg^{-1} (energy density) and power density of about 411 W kg^{-1} for 1 A g^{-1}, outperforming other composite samples.

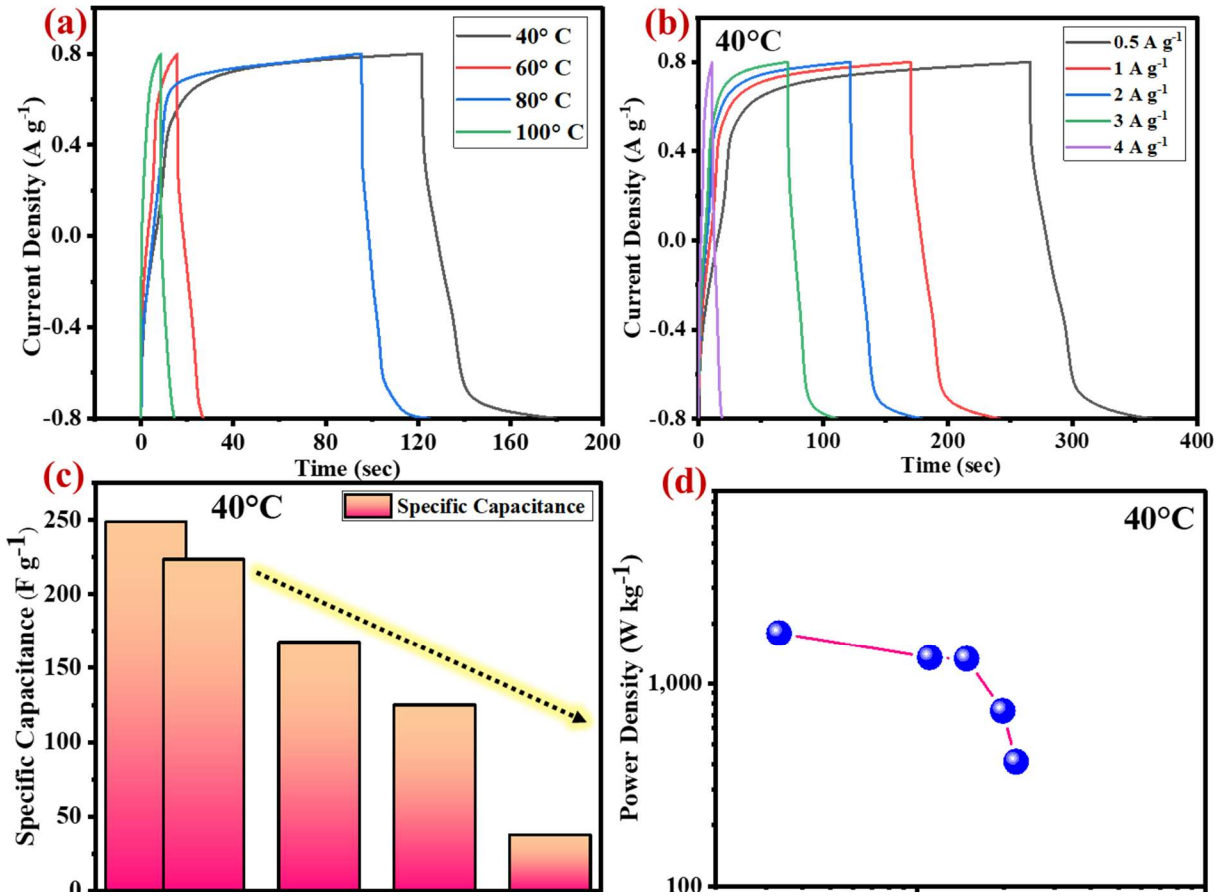

Figure 6. (a) GCD plot for the sample at unlike temperature (40-120˚C), (b) GCD for CAC-40 at dissimilar current density, (c) specific capacitance change vs current density, and (d) Ragone graph for CAC-40 sample.

Table 1. Different electrochemical parameters for CAC-40 samples at different current densities

Current Densities ($A\ g^{-1}$)	Specific Capacitance ($F\ g^{-1}$)	Energy Density ($Wh\ kg^{-1}$)	Power Density ($W\ kg^{-1}$)
0.5	248	22	411
1	223	20	733
2	167	15	1329
3	125	11	1347
4	37	3	1786

The resistive and capacitive properties of the organized composites were investigated using EIS for frequency shifting from 0.1 Hz- 0.1 MHz. The Nyquist plots for all samples are revealed in **Fig. 7a**, highlighting two distinct frequency regions: (a) the high-frequency region, which exhibits a semicircle. The intersection of this semicircle with the X-axis, along with its diameter, represents the charge transfer resistance (R_{ct}) and bulk resistance; (b) the region of low-frequency, depicts a line that appears parallel to the Y-axis.

The bulk resistance (R_b) reflects the resistance within the cell, including interfaces and solvents. **Fig. 7b** presents a bar graph comparing the R_b and R_{ct} resistances of all samples at different temperatures. It reveals that the CAC-40 sample has the lowest bulk resistance ($R_b = 5.3\ \Omega$) also $R_{ct} = 0.9\ \Omega$ relative to other samples at varied temperatures. This low bulk resistance suggests that the CAC-40 material offers an efficient, unobstructed pathway for ion transport, promoting optimal charge storage.

In the proposed research, the functional properties of activated carbon will be thoroughly examined and incorporated to understand its impact on energy storage device performance. Activated carbon is widely recognized for its high surface area, excellent porosity, and stability, making it a valuable additive in energy storage systems, particularly for enhancing electrode performance. The study aims to explore how incorporating activated carbon into cobalt diselenide electrode materials can improve critical performance metrics such as electrochemical stability, energy density, and power density. Also, the incorporation of activated carbon and cellulose fibers significantly enhanced the electrochemical performance of the composite, resulting in a substantial increase in specific

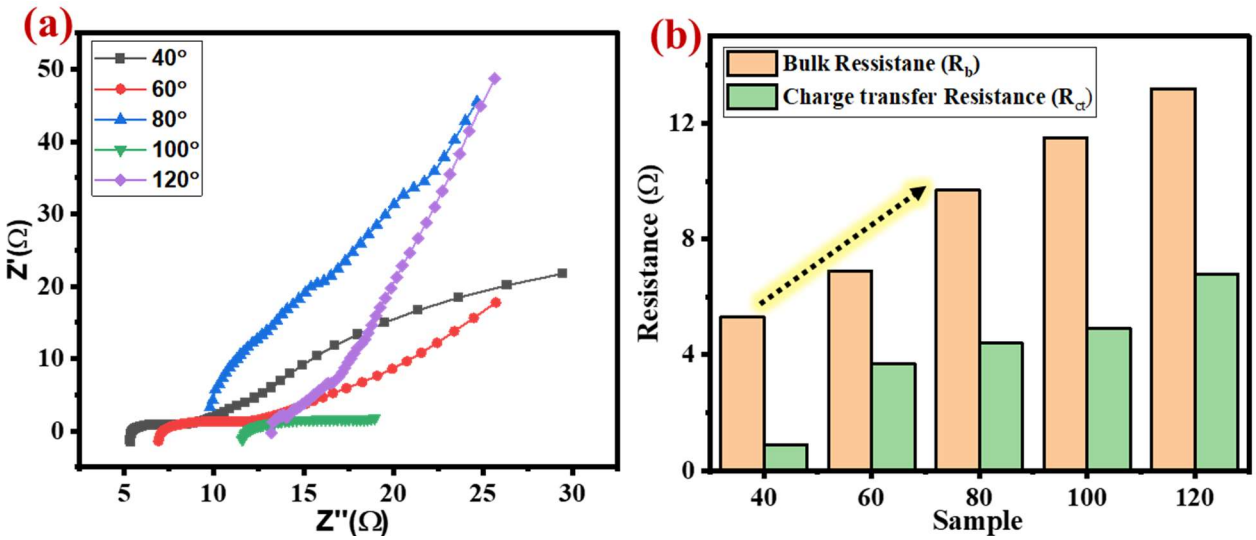

Figure 7.(a) Nyquist plot, and (b) bar graph indicating bilk and charge transfer resistance for the cell at different temperatures.

capacitance and improved charge-discharge kinetics.

4. Conclusion

This study successfully demonstrates the electrochemical behavior of a cobalt diselenide ($CoSe_2$) --based ternary composite hybrid supercapacitor across varying temperatures. The electrode material depicted surface is about 460 m^2 g^{-1}. The incorporation of activated carbon and cellulose fibers significantly enhanced the electrochemical performance of the composite, resulting in a substantial increase in specific capacitance and improved charge-discharge kinetics. The composite-based cell at 40˚ C temperature revealed a specific capacitance of 248 F g^{-1}, which further decreased at higher temperatures, showcasing a negative correlation between temperature and electrochemical performance. The energy and power densities obtained for the same electrode are estimated at around 22 Wh kg^{-1} and 411 W kg^{-1}. Our findings reveal that the specific capacitance of the supercapacitor decreased with temperature, highlighting the negative impact of elevated temperatures on the ion's mobility and charge transfer efficiency. These results suggest that the ternary composite not only enhances energy storage capacity but also ensures reliable performance over extended use. Overall, the findings of this research indicate the promising potential of $CoSe_2$-based ternary composites for high-performance energy storage applications at around room temperature. Future research may focus on optimizing the composite's morphology and exploring additional synergistic materials to further enhance performance.

CReDiT authorship contribution statement

Shweta Tanwar: Conceptualization, Formal analysis, Investigation, Validation, Methodology, Visualization, Writing-Original draft, review, and editing. **Nirbhay Singh**-Investigation, Validation, Visualization, Writing- review, and editing. **Anurag Gaur**-Conceptualization, Visualization, Investigation, Supervision, Writing- review, and editing. **A. L. Sharma**: Visualization, Investigation, Writing-review, and editing, Supervision.

Declaration of Competing Interest

The authors declare that they have no known competing financial interests or personal relationships that could have appeared to influence the work reported in this paper.

Acknowledgments

One of the authors, Shweta Tanwar acknowledges the SERB (DST, Govt, of India) for the award of the National Post Doctoral Fellowship (NPDF) (PDF ID-PDF/2023/001001) fellowship. The authors also acknowledge the Central Instrumentation Laboratory, Central University of Punjab for material characterization facilities.

References

[1] Tanwar S, Singh N, Sharma AL. Cellulose-doped ternary composites for high-performance hybrid supercapacitor. Mater Res Bull 2024:113033.

[2] Tanwar S, Sharma AL. Insight into use of biopolymer in hybrid electrode materials for supercapacitor applications—A critical review. J Appl Phys 2023;133.

[3] Pateriya RV, Tanwar S, Sharma AL. Carbon decorated Li-based orthosilicate electrode for energy storage application. J Mater Sci 2024:1–18.

[4] Tanwar S, Arya A, Gaur A, Sharma AL. Transition metal dichalcogenide (TMDs) electrodes for supercapacitors: a comprehensive review. J Phys Condens Matter 2021;33:303002. https://doi.org/10.1088/1361-648x/abfb3c.

[5] Tanwar S, Singh N, Kour S, Sharma AL. Investigation of temperature effect on the electrochemical performance of MoSe2@ FeOOH composite. AIP Conf. Proc., vol. 2995,

AIP Publishing; 2024.
[6] Singh N, Tanwar S, Sreehari MS, Sharma AL, Yadav BC. An approach to substitute costly-commercial capattery electrodes by activated carbon@ Co with advanced retention: Detailed device study supported by DFT investigation. J Energy Storage 2024;80:110244.
[7] Kour S, Tanwar S, Singh N, Sharma AL. Electrochemical performance of ZnCo2O4 nanosheets in aqueous electrolytes for supercapacitor applications. AIP Conf. Proc., vol. 2995, AIP Publishing; 2024.
[8] Sarathi MTV, Tanwar S, Sreehari MS, Mondal K, Sharma AL. Surfactants effect on the electrochemical properties of FeSe2 electrode for supercapacitor with first principles insights into quantum capacitance. Ceram Int 2024;50:7266–80.
[9] Singh N, Tanwar S, Kumar P, Sharma AL, Yadav BC. Advanced sustainable solid state energy storage devices based on FeOOH nanorod loaded carbon@ PANI electrode: GCD cycling and TEM correlation. J Alloys Compd 2023;947:169580.
[10] Tanwar S, Singh N, Vijayan AK, Sharma AL. Electrochemical performance investigation of different shaped transition metal diselenide materials based symmetric supercapacitor with theoretical investigation. Surfaces and Interfaces 2023;42:103504.
[11] Chen T, Li S, Gui P, Wen J, Fu X, Fang G. Bifunctional bamboo-like CoSe2 arrays for high-performance asymmetric supercapacitor and electrocatalytic oxygen evolution. Nanotechnology 2018;29:205401.
[12] Singh N, Tanwar S, Sharma AL, Yadav BC. Economic and environment friendly carbon decorated electrode for efficient energy storage devices. J Energy Storage 2023;66:107452.
[13] Yu N, Zhu M-Q, Chen D. Flexible all-solid-state asymmetric supercapacitors with three-dimensional CoSe 2/carbon cloth electrodes. J Mater Chem A 2015;3:7910–8.
[14] Tanwar S, Singh N, Sharma AL. Fabrication of Activated Carbon coated MSe2 (M= Mo, Co, and Ni) Nanocomposite Electrode for High-Performance Aqueous Asymmetric Supercapacitor. Colloids Surfaces A Physicochem Eng Asp 2023:131235.
[15] Tanwar S, Singh N, Sharma AL. Structural and electrochemical performance of carbon coated molybdenum selenide nanocomposite for supercapacitor applications. J Energy Storage 2022;45:103797.
[16] Tanwar S, Singh N, Sharma AL. High-performance different shape carbon decorated asteroidea-like cobalt diselenide electrode for energy storage device. Fuel 2022;330:125602. https://doi.org/https://doi.org/10.1016/j.fuel.2022.125602.
[17] Ariponnammal S, Velvizhi R. Structural, EPR, magnetic and photoluminescence studies on cobalt selenide. Invertis J Sci Technol 2016;9:1–5.
[18] Mojoudi N, Mirghaffari N, Soleimani M, Shariatmadari H, Belver C, Bedia J. Phenol adsorption on high microporous activated carbons prepared from oily sludge: equilibrium, kinetic and thermodynamic studies. Sci Rep 2019;9:1–12.
[19] Manigandan R, Giribabu K, Suresh R, Vijayalakshmi L, Stephen A, Narayanan V. Cobalt oxide nanoparticles: characterization and its electrocatalytic activity towards nitrobenzene. Chem Sci Trans 2013;2:S47–50.